Electron Dynamics Driven by Light-Pulse Derivatives

Qi-Cheng Ning, Ulf Saalmann, and Jan M. Rost

Max Planck Institute for the Physics of Complex Systems, Nöthnitzer Straße 38, 01187 Dresden, Germany

We demonstrate that ultrashort pulses carry the possibility for a new regime of light-matter interaction with nonadiabatic electron processes sensitive to the envelope derivative of the light pulse. A standard single pulse with its two peaks in the derivative separated by the width of the pulse acts in this regime like a traditional double pulse. The two ensuing nonadiabatic ionization bursts have slightly different ionization amplitudes. This difference is due to the redistribution of continuum electron energy during the bursts, negligible in standard photoionization. A time-dependent close-coupling approach based on cycle-averaged potentials in the Kramers-Henneberger reference frame permits a detailed understanding of light-pulse derivative-driven electron dynamics.

With increasingly shorter pulses becoming available in the optical and vacuum ultraviolet domain, it has been noticed that the light-pulse envelope influences the outcome of experiments. Most widely known is the influence of the carrier envelope phase quantifying the shift of the periodic carrier wave relative to the maximum of the pulse envelope [1]. Also, effects of the spatial envelope dependence beyond the dipole approximation of light-matter coupling [2,3] and a chirp on the ultrashort pulse [4] have been pointed out. A more indirect effect is induced by the time-dependent ac-Stark shift of energy levels which follows the pulse envelope. It gives rise to dynamic interference [5,6], termed as such and elegantly explained in Refs. [7,8]. Inspired by earlier work [5], the envelope Hamiltonian was introduced [9], which explicitly separates the optical periodic time dependence from that of the envelope variation and permits therefore a clear distinction of multiphoton [10] and nonadiabatic [11] ionization under short pulses. Much earlier and on much longer time scales of Rydberg excitation and femtosecond pulses, pulse envelope effects, mostly in connection with transient Stark shift enabled resonances, were pointed out [12–17].

Despite these various notions on effects of the pulse envelope, the simple but dramatic consequences for nonadiabatic ionization and the possibilities these consequences carry have not yet been addressed: Plainly put, in the regime of extreme nonadiabatic matter-light coupling, electron dynamics becomes sensitive to the light-pulse derivatives. Hence, a standard Gaussian laser pulse acts as a double pulse through the two peaks of its derivative. With the Gaussian pulse as an example, we will establish that, in general, nonadiabatic electron dynamics is sensitive to the pulse envelope derivative (PED) of the laser pulse rather than to the envelope (maximum) itself.

Nonadiabatic dynamics occurs for states which change fast as a function of an external parameter [18]. Molecules

are the most widely known examples, where the electronic Born-Oppenheimer states depend parametrically on the nuclear positions. In the present context, we formulate the electronic state as parametrically dependent on the pulse envelope. The ensuing nonadiabatic ionization is exclusively due to PED, as we will see below. Therefore, nonadiabatic ionization is complementary to dynamic interference, resonant population trapping, or Rydberg multiphoton ionization [7,12–17]. These are adiabatic phenomena in the sense that a resonance condition for an energy difference of bound states, well defined at each time during the pulse, is fulfilled twice, during the rise and fall of the pulse, respectively. These two times are, in general, not where the envelope derivative peaks, as is the case for nonadiabatic ionization. Moreover, the resonant effects mask nonadiabatic ionization and its low-energy photoelectron peak, as we discuss here. Otherwise, nonadiabatic ionization could have already been identified in the 1990s, in particular, in Rydberg experiments such as Ref. [17].

To demonstrate that nonadiabatic ionization is indeed sensitive only to the *change* of the pulse envelope, we will consider a pulse with a short rise and fall encompassing a plateau of variable duration T_c. This allows us to analyze and understand the subtle differences of the beginning and the end of the pulse separately and to demonstrate that illumination with a maximal amplitude during the plateau has no effect on nonadiabatic ionization. Shrinking the plateau to $T_c = 0$, we will arrive at the normal single ultrashort pulse, whose effect is then easily understood in terms of the (already analyzed) rising and falling part of the pulse.

Although the envelope-derivative effects we are going to investigate are independent of the theoretical description, we deliberately choose the envelope Hamiltonian [9], since it reveals in connection with a time-dependent close-coupling (CC) representation the mechanism of envelope-driven nonadiabatic electron dynamics, including subtle effects

033203-1

such as the reshuffling of electron energy in the continuum. To this end, we Fourier expand the periodic time dependence of the electron potential $V(\mathbf{x}, t)$ in the Kramers-Henneberger frame, keeping the time evolution of the pulse envelope explicit [atomic units (a.u.) are used unless stated otherwise]:

$$V_n(\mathbf{x}, t) = \frac{\omega}{2\pi} \int_0^{2\pi/\omega} e^{in\omega t'} V(\mathbf{x} + \alpha(t)\mathbf{e}_z \cos(\omega t' + \varphi)) dt', \tag{1}$$

where $\mathbf{x}_\omega(t) = \alpha(t)\mathbf{e}_z \cos(\omega t + \varphi)$ can be understood as the trajectory of a free electron in the laser electrical field linearly polarized along $\mathbf{e}_z$ and defined by the second derivative of $\mathbf{x}_\omega(t)$. While to a very good accuracy an expansion length of $n_{\max} = 2$ is sufficient in the potentials (1) as shown before [9], nonadiabatic dynamics sensitive to the envelope derivative $d\alpha/dt$ is mainly described through $V_0(\mathbf{x}, t)$ with eigenstates and energies parametrically dependent on time in

$$[H_0(t) - E_\beta(t)]|\psi_\beta(t)\rangle = 0, \tag{2}$$

where $H_0 = -\frac{1}{2}\nabla^2 + V_0$.

This is directly illustrated for a flattop pulse in Fig. 1. It is constructed from a Gaussian pulse extended by inserting at its maximum a plateau of length T_c; see Fig. 1(a). To keep the analysis as simple as possible, we use a one-dimensional model potential for a weakly bound electron introduced in different contexts before [19] as a specific example. We compare the photoelectron spectrum obtained from the solution of the time-dependent Schrödinger equation (TDSE) with the full Hamiltonian and with H_0. Both solutions agree quite well for slow electrons $E/\omega \ll 1$

[compare lines and symbols in Fig. 1(b)] implying a nonadiabatic regime with envelope-derivative-driven electron dynamics. Since this derivative has two peaks during the rise and fall of the pulse, respectively, but vanishes during the plateau of the pulse, we expect two ionization bursts which generate a typical two-slit interference pattern as a function of plateau length T_c in the electron spectrum:

$$P_E(T_c) = a_E \cos(\varphi_E - \delta_E T_c) + c_E. \tag{3}$$

Indeed, for any fixed energy E the ionization yield oscillates perfectly as a function of plateau length T_c, as shown in Fig. 1(b). Fitting (3) to these yields, we can extract φ_E and δ_E, which allows us to determine from

$$\varphi_E - \delta_E T_c = n\pi \tag{4}$$

the maxima (n even, dashed line) and minima (n odd, solid line) in very good agreement with the numerical spectra as shown in Fig. 1(c). In the (E, T_c) plane, the functional form $T_c \propto E^{-1}$ of these extrema follows directly from the difference between the final and initial energy, $\delta_E = E - E_g^\star$. Note, however, that, in contrast to standard double pulses, the light pulse illuminates the target with the maximal amplitude between the (nonadiabatic) ionization bursts. Therefore, $E_g^\star$ is the initial energy dressed by the laser field, as indicated by the star.

As a next step, we take a closer look at the ionization bursts themselves. The fast rising and falling half-pulses generate the electron spectra shown in Figs. 2(e) and 2(f) with solid lines, respectively. We have obtained these spectra by *wave-packet partitioning*: We solve the TDSE for H_0 with the electron initially in the ground state
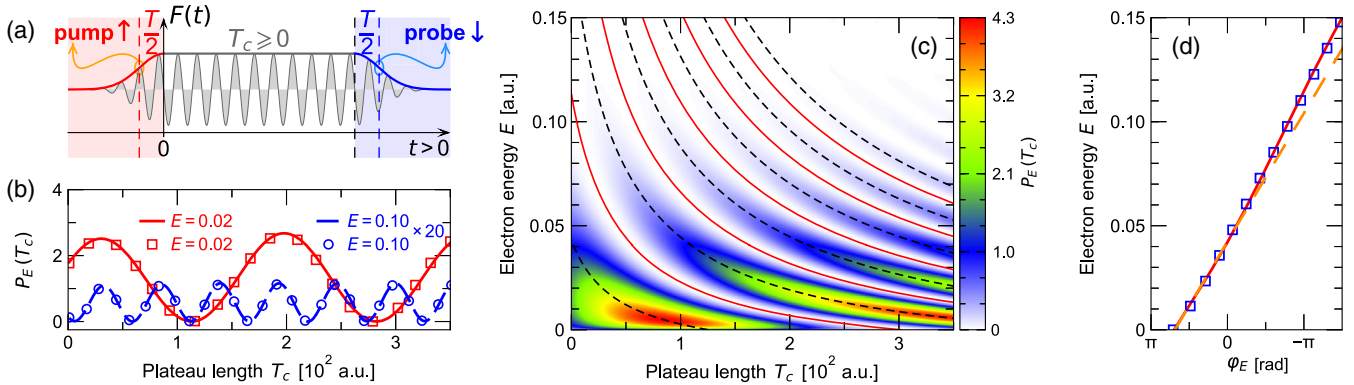
FIG. 1. Nonadiabatic ionization. (a) A flattop laser pulse rising (↑) and falling (↓) over a time span of $T/2 = 25.5$ a.u. between the maximum of the electric field amplitude $F(t)$ and its maximal derivative. These two Gaussian half pulses, which act similarly as a pump and probe pulse in the nonadiabatic regime, encompass a plateau of duration T_c. (b) Electron spectra for two energies as a function of plateau length T_c for an electron initially bound by a weak potential at energy $E_g = -0.0277$ a.u. exposed to a laser pulse of peak amplitude $F = 0.5$ a.u. and frequency $\omega = 0.314$ a.u.; see the text. TDSE solutions with the full Hamiltonian are given as lines and with H_0 from Eq. (2) as symbols. (c) Nonadiabatic electron spectrum $P_E(T_c)$. The lines mark the maxima and minima predicted from Eq. (4). (d) Phase difference φ_E, extracted by fitting Eq. (3) to spectra for fixed E as in (b) (symbols); from benchmark calculations obtained through wave-packet partitioning (see the text) for the Gaussian pulse, i.e., $T_c = 0$ (solid line); and approximated with Eq. (7) (dashed line).
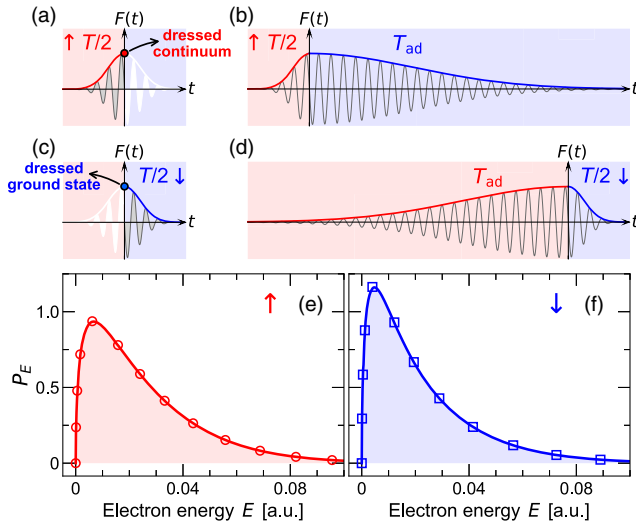
FIG. 2. Nonadiabatic electron spectra from Gaussian half-pulses. (a) Sketch of the partitioning approach for the rising ($\uparrow$) half-pulse. (b) The artificial laser field with the falling pulse length T_{ad} long enough to not affect nonadiabatic dynamics while the rising part has as before $T/2 = 25.5$ a.u. (Note that for the figure sketch $T_{ad} = 170$ a.u., while in the calculations $T_{ad} = 850$ a.u. has been used, which is sufficiently long to obtain converged results.) (e) The photoelectron spectrum from the partitioning approach as sketched in (a) (lines) and from the artificial laser field as in (b) (symbols). (c), (d), and (f) show information analogous to (a), (b), and (e), respectively, but for the falling ($\downarrow$) half-pulse instead of the rising half-pulse. The peak field strength and laser frequency are the same as in Fig. 1.

$\psi_g(t \to -\infty)$. Projecting at the end of the rising half-pulse at $t = 0$ onto the instantaneous continuum eigenstates ψ_E of H_0 at the maximal field [Fig. 2(a)], we obtain the spectrum of the first burst [Fig. 2(e)]. For the falling half-pulse we begin the propagation in the (dressed) ground state $\psi_g^\star$ at the maximal field [Fig. 2(c)] and obtain the spectrum of the second burst from $\psi_E(t \to \infty)$; see Fig. 2(f). Underscoring again the nonadiabatic dynamics, the result is the same [see the solid lines in Figs. 2(e) and 2(f)] if we amend the left half-pulse with a slowly decaying tail [half width $T_{ad} = 850$ a.u., Fig. 2(b)] and start the right half-pulse with an equally slow rise [$T_{ad} = 850$ a.u., Fig. 2(d)]. Since the concatenation of the two half-pulses should be identical to our pulse for $T_c = 0$, i.e., a Gaussian pulse, we expect that the phase φ_E in (3) is given by the phase difference $\varphi_E = \varphi_\uparrow(E) - \varphi_\downarrow(E)$ of the two burst amplitudes $A_{\uparrow\downarrow}(E)e^{i\varphi_{\uparrow\downarrow}(E)}$. This is indeed the case, as shown in Fig. 1(d). Note that, suitable for nonadiabatic dynamics, we measure the amplitude pulse length T here as the time span between the maxima in the derivative of the pulse envelope which is related to the standard measure of full width at half maximum (FWHM) of the envelope τ through $T = \tau/(2\ln 2)^{1/2} = 0.85\tau$.

Interestingly, the electron spectra from the rising ($\uparrow$) and falling ($\downarrow$) half-pulse differ slightly, although the

total (energy-integrated) ionization yield is the same, in our example $P_\uparrow \equiv \int A_\uparrow^2(E)dE = P_\downarrow \equiv \int A_\downarrow^2(E)dE = 0.03247$ a.u. [20]. This suggests that absorption from the initial state does not depend on the character of the half-pulse (rising or falling), while there must be a mechanism of redistributing energy in the continuum, sensitive to the sign of the pulse derivative. In contrast to the fully numerical solutions presented so far, a CC representation in a basis allows us to distinguish nonadiabatic bound-continuum M_{Eg} from continuum-continuum $M_{EE'}$ transitions, with the transition matrix elements

$$M_{E\beta}(t) = \frac{\langle \psi_E(t) | \partial_t V_0(\mathbf{x}, t) | \psi_\beta(t) \rangle}{E - E_\beta(t)} \quad (5)$$

for both cases. Inserting the wave function $|\Psi(t)\rangle = \oint_\beta |\psi_\beta(t)\rangle e^{-i\int^t E_\beta(t')dt'} c_\beta(t)$ into the TDSE with the Hamiltonian $H_0(t)$, the matrix elements (5) govern the evolution of the time-dependent amplitudes $c_\beta(t)$ through [9]

$$\frac{dc_g}{dt} = -\int_0^\infty c_E M_{Eg} e^{-i\phi_g} dE, \quad (6a)$$

$$\frac{dc_E}{dt} = c_g M_{Eg} e^{i\phi_g} + \int_0^\infty c_{E'} M_{EE'} e^{i\phi_{E'}} dE' \quad (6b)$$

with the phases

$$\phi_\beta(t) = \int^t [E - E_\beta(t')]dt' \quad (6c)$$

for the ground state $\beta = g$ or a continuum state with energy $\beta = E'$, respectively. Note that $M_{E\beta}$ is real and $M_{EE} = 0$.

As expected, the CC spectra for the left and right half-pulses are indistinguishable from our full numerical spectra obtained by wave-packet partitioning; see Fig. 3. If we, however, calculate the left and the right spectra without the continuum-continuum coupling $M_{EE'}$ in Eqs. (6), they become identical (see the dashed-dotted curves in Fig. 3) and still produce the same total ionization yield as in the full calculation. Consequently, the already ionized (continuum) electrons are redistributed towards higher energy through $M_{EE'}$ during the rising half-pulse while being reshuffled towards lower energy in the continuum for the falling half-pulse. This explains the difference in the two burst spectra. The *continuum energy reshuffling* is another (subtle) effect of PED-induced electron dynamics. It is absent in traditional double pulses with a slowly varying envelope, since for those pulses the matrix element $M_{EE'}$ will be negligible.

Following our argument so far, the electron spectrum (3) for a single Gaussian pulse ($T_c = 0$) is composed from the coherent superposition of the slightly different burst amplitudes. Since they are created close to the maxima of the
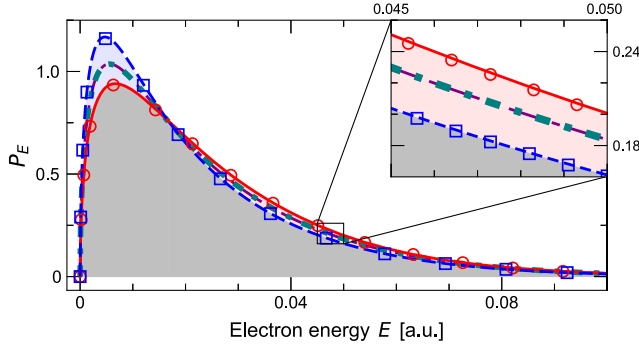
FIG. 3. Energy reshuffling of continuum electron wave packets. Photoelectron spectra from the rising (red) and falling (blue) half-pulses. Results are obtained by the CC equations (6) with (solid and dashed lines) and without (dashed-dotted lines) the continuum coupling contribution $M_{EE'}$, as well as with wave-packet partitioning (symbols). The laser parameters are the same as in Fig. 1.

FIG. 4. The nonadiabatic electron spectrum of a single Gaussian pulse of width $T = 51$ a.u. (dashed-dotted line) and combined from the sequence of a rising and falling half-pulse with $T/2 = 25.5$ a.u. (open circles). In addition the contribution from the first electron burst $\tilde{A}_\uparrow{}^2(E)$ (solid, red line) and the second one $A_\downarrow{}^2(E)$ (dashed blue line) are shown. The inset reveals Stueckelberg oscillations [21] of the normalized spectrum, $\bar{P}_E \equiv P_E/[2\tilde{A}_\uparrow{}^2(E) + 2A_\downarrow{}^2(E)]$. The laser parameters are the same as in Fig. 1.

envelope derivative at times $\pm T/2$, their phases differ during the interval T between the two bursts, and therefore the phase difference in Eq. (4) may be approximated using Eq. (6c) as

$$\varphi_E = -ET + \int_{-T/2}^{+T/2} E_g(t)dt + \pi, \qquad (7)$$

where π is a consequence of the opposite sign of the two burst amplitudes. One sees in Fig. 1(d) that Eq. (7) describes φ_E well, in particular, for small energies E.

There is, however, one last element missing, namely, that the first electron burst amplitude $A_\uparrow(E)$ gets modified by the second half-pulse to $\tilde{A}_\uparrow(E)$ in that energy is shuffled through $M_{EE'}$ towards lower energies, partially canceling the continuum shuffling during the first half-pulse towards higher energies. As a result, the spectra of the two electron bursts are more similar when combined in a full pulse (blue and red curves in Fig. 4) than if considered separately as in Figs. 2 and 3. Still, the two burst amplitudes are not identical after the end of the pulse, apart from a single point in energy $E \approx 0.02$ a.u. where they cross. As expected from the phase difference φ_E, the two burst amplitudes interfere and produce oscillations in the spectrum as a function of energy E. Since their period is larger than the energy interval covered by the nonadiabatic ionization peak, it is necessary to normalize the spectrum with its major variation in energy in order to uncover the oscillations; see the inset in Fig. 4. Hence, our analysis of nonadiabatic ionization in terms of electron bursts induced by half-pulses has lead us to a surprising reinterpretation of the photoelectron spectrum at low energies (gray area in Fig. 4) including the identification and explanation of an oscillatory structure, clearly visible in the normalized spectrum $\bar{P}_E$.

We finally come back to the modification of the first burst by the second half-pulse, which is also known from standard double pulses in the adiabatic regime. It simply

means that the wave packet of the first burst is still in the vicinity of the potential with range d during the second half-pulse. Modifications are expected if $d/D \equiv d/\sqrt{2E_{\text{peak}}}/T < 1$, where D is the distance traveled by the continuum wave packet during the time T elapsed between the two bursts, estimated from its most probable energy E_{peak}. Note that here T is just the width of the single short (Gaussian) pulse. With the flattop pulse we have introduced in the beginning, we can probe the evolution of the modification, since there the time between bursts is given by $T + T_c$. Indeed, the modification of the first burst vanishes for a long plateau as one can see in Fig. 5.

In summary, in the regime of nonadiabatic light-matter interaction, electron dynamics is sensitive to the envelope derivative of a light pulse. Therefore, a typical short Gaussian pulse acts like a "double pulse" through its two maxima in the envelope derivative, separated by $T = 0.85\tau$, where τ is the
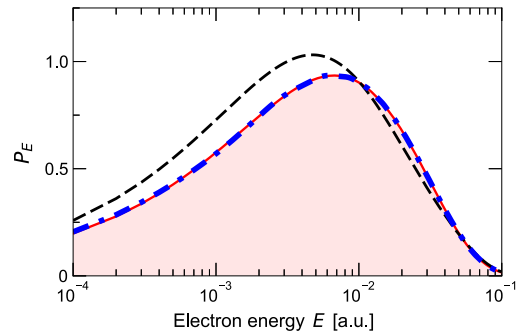
FIG. 5. Photoelectron spectrum $A_\uparrow{}^2(E)$ of a rising half-pulse only as in Fig. 2(e) (solid red line) and $\tilde{A}_\uparrow{}^2(E)$ modified by the falling half-pulse for different plateau lengths T_c ($T_c = 0$, dashed black line; $T_c = 2000$ a.u., dashed-dotted blue line). The laser parameters are the same as in Fig. 1.

FWHM of the Gaussian envelope. It creates two ionization bursts, which can also be interpreted as being composed from two ionization paths for each final electron energy E. Between the two bursts, some electron amplitude of the first path is already in the continuum, while the one of path two is still in the (laser-dressed) ground state. This gives rise to a phase difference proportional to the energy difference of the two paths and the time T over which this energy difference exists and leads to an interference structure in the nonadiabatic part of the electron spectrum produced by a single short Gaussian pulse. Another subtle feature is the energy reshuffling in the continuum which has the opposite effect on bursts produced by the rising and falling half-pulse, respectively.

Clearly, nonadiabatic short-pulse-induced electron dynamics carries unusual features which we have described here. They can occur whenever the pulse envelope changes on the relevant electronic time scale. They will be most prominent for ultrashort pulses, where resonant excitation is less likely to dominate. Sensitive to the derivative of the pulse envelope, these features provide new avenues to coherently steer electron dynamics when light-pulse derivatives can be controlled.

[1] G. G. Paulus, F. Grasbon, H. Walther, R. Kopold, and W. Becker, Phys. Rev. A **64**, 021401 (2001).

[2] M. Førre, S. Selstø, J. P. Hansen, and L. B. Madsen, Phys. Rev. Lett. **95**, 043601 (2005).

[3] A. S. Simonsen, T. Kjellsson, M. Førre, E. Lindroth, and S. Selstø, Phys. Rev. A **93**, 053411 (2016).

[4] H.-C. Shao and F. Robicheaux, Phys. Rev. A **93**, 053414 (2016).

[5] K. Toyota, O. I. Tolstikhin, T. Morishita, and S. Watanabe, Phys. Rev. A **76**, 043418 (2007).

[6] K. Toyota, O. I. Tolstikhin, T. Morishita, and S. Watanabe, Phys. Rev. A **78**, 033432 (2008).

[7] P. V. Demekhin and L. S. Cederbaum, Phys. Rev. Lett. **108**, 253001 (2012); Phys. Rev. A **88**, 043414 (2013).

[8] Although the idea is correct, the articles of Ref. [7] contain flaws rendering their results invalid, see M. Baghery, U. Saalmann, and J. M. Rost, Phys. Rev. Lett. **118**, 143202 (2017).

[9] K. Toyota, U. Saalmann, and J. M. Rost, New J. Phys. **17**, 073005 (2015).

[10] D. Meshulach and Y. Silberberg, Phys. Rev. A **60**, 1287 (1999).

[11] K. Toyota, O. I. Tolstikhin, T. Morishita, and S. Watanabe, Phys. Rev. Lett. **103**, 153003 (2009).

[12] K. Schafer and K. Kulander, Laser Phys. **7**, 740 (1997).

[13] R. R. Freeman, P. H. Bucksbaum, H. Milchberg, S. Darack, D. Schumacher, and M. E. Geusic, Phys. Rev. Lett. **59**, 1092 (1987).

[14] J. G. Story and T. F. Gallagher, Phys. Rev. A **47**, 5037 (1993).

[15] J. G. Story, D. I. Duncan, and T. F. Gallagher, Phys. Rev. Lett. **70**, 3012 (1993).

[16] J. G. Story, D. I. Duncan, and T. F. Gallagher, Phys. Rev. A **50**, 1607 (1994).

[17] R. R. Jones, Phys. Rev. Lett. **74**, 1091 (1995).

[18] H. Nakamura, *Nonadiabatic Transition: Concepts, Basic Theories and Applications* (World Scientific, Singapore, 2012).

[19] A. M. Popov, O. V. Tikhonova, and E. A. Volkova, J. Phys. B **32**, 3331 (1999).

[20] One can show, in general, that two pulses $f(t)$ and $f(-t)$ induce the same depletion of the initial state. Since the system considered here has just one bound state and $F_\uparrow(t) = F_\downarrow(-t)$ (see, e.g., Fig. 2), this implies $P_\uparrow = P_\downarrow$.

[21] E. C. G. Stueckelberg, Helv. Phys. Acta **5**, 369 (1932).